Hindawi
Mathematical Problems in Engineering
Volume 2018, Article ID 7246503, 11 pages
https://doi.org/10.1155/2018/7246503

Research Article

Research on 3D Modeling Method of Cobblestone Road Based on Geometric Characteristics

Jinhua Han,[1] **Ke Feng**,[1] **Huanliang Li**,[1] **Hongxin Cui**,[1] **and Jing Chen**[2]

[1]*College of Field Engineering, Army Engineering University of PLA, Nanjing 210007, China*
[2]*Unit 61489, PLA, Luoyang 471023, China*

Correspondence should be addressed to Ke Feng; fengke0430@163.com

Received 29 December 2017; Accepted 17 May 2018; Published 27 June 2018

Academic Editor: Denis Benasciutti

Based on the analysis of the geometric characteristics, distribution characteristics, and constraints of the cobblestone road, a three-dimensional (3D) parametric road modeling method based on geometric characteristics is proposed. The cobblestone model is established by the exponential oval equation, and the cobblestones distribution is determined by Monte Carlo stochastic search method. Then the 3D theoretical model of cobblestone road is obtained. To veritably simulate the cobblestone road, a generated 3D random road is fusing with the 3D cobblestone road model by alternating values, and the comparison between the real and modeling cobblestone roads is done in space domain and PSD curves. Then based on the establishment of the standard vehicle vibration model, the influences of the key geometric parameters of the cobblestone road on the vehicle vibration are analyzed by using the evaluation indices of the IRI and the RMS of the vehicle body acceleration. The proposed method can be extended to the 3D modeling of almost all strengthened test roads such as Belgian road, fish-scale pits road, ripple tracks, and washboard road and provides a 3D road modeling method with adjustable parameters, authenticity, and accuracy for the comprehensive construction of vehicle virtual test field.

1. Introduction

With the rapid development and update of the vehicle, compared with the real vehicle driving test [1], the vehicle road simulation test [2] and virtual road test [3] have attracted more and more attention in automotive engineering field in recent years with the advantages of time-saving, low costs, high accuracy, repeatability, controllability, and so forth.

Road profile [4] is the most important external excitation of the ground vehicle, which influences vehicle ride comfort, operational stability, driving reliability, fatigue life of components, and so forth. With the excitation of road roughness on the vehicle, the vehicle is affected by the external forces and the internal forces of the vehicle itself, which are changing over time. When the vehicle is running through the road, the vehicle's components are always bearing the stress and strain, which would result in fatigue and failure after a certain mileage [5]. The worse the road condition is, the faster the fatigue failure of vehicle parts is. Therefore, providing accurate road profile for vehicle reliability testing and simulation has been an important research content in this field.

Currently, the methods of road profile acquisition [6] at home and abroad mainly include direct measurement method and simulation method [7]. Among them, the direct measurement methods of road profile had formed many measuring methods and corresponding equipment in long-term research [8, 9], including Level and Rod, Multiwheel Profilograph, BPR Roughometer, Inertial Profiler, and Laser Profiler. The Level and Rod is the earliest method of road profile measurement and has been used in the construction and acceptance process of airport runway in Europe and America and various automobile proving grounds in China [10]. The Level and Rod method has high accuracy, but the measuring speed is too slow, which is mainly used for calibration of other measuring instruments now. In order to improve the efficiency of measurement, the Multiwheel Profilograph, BPR Roughometer, and Inertial Profiler are applied. But these measuring instruments are difficult to take account of the speed and accuracy simultaneously.

Then the application of laser sensor makes the laser profiler achieve high speed and accurate measurement of the road and becomes a widely used measurement method. Although the direct measurement methods can obtain a more accurate road profile, only a single road trajectory is obtained, which cannot be used for virtual test based on 3D model.

The simulation methods can reconstruct the required road profiles according to the statistical characteristics of road roughness, which contain harmonic superposition method [11], filtered white noise method, AR (ARMA) method, fast Fourier inversion generation method, and so forth [12, 13]. However, these road profile reconstruction methods [14] are based on the theory of stationary random process, which can only produce stochastic histories of stationary Gauss distribution. The above methods are difficult to reconstruct the road profile of the strengthened roads in the vehicle proving ground accurately, which have evident non-Gaussian characteristics [15, 16].

In terms of modeling of road geometry, 3D models can more accurately reflect the effect of roads on vehicles, especially when vehicles are subjected to lateral loading; thus more accurate test results are obtained in the virtual test based on 3D model [17, 18]. The application of laser scanning technology makes it possible to measure the 3D road profile directly and accurately. General Motors used an industrial 3D laser scanning instrument to build the high-precision models for the test ground roads in 2011, but the instrument is huge, expensive, and inefficient. And the portable 3D laser scanner for road 3D scanning requires multistation scanning and point cloud splicing with a low efficiency. Then some studies are done to reconstruct 3D road model. C. Cheng et al. [19] presented a new way to create 3D virtual road by calculating the connections of each code with the Delaunay triangulation algorithm based on the ADAMS software. Based on the measured trajectory of the middle route of the road, the road profile is reconstructed with the interpolation method in [20, 21], and the comparative analysis of the reconstructed roads in Regular Grid Road (RGR), Curved Regular Grid (CRG), and Triangular Mesh Road Definition File (RDF) formats is made in the simulation efficiency. However, the above road modeling methods are completed on the basis of the measured road profile data, combined with the characteristics of the road profile, and they are not comprehensive for describing the geometric characteristics of the road.

In all kinds of strengthened test roads, such as long/short ripple tracks, washboard road, Belgian road, cobblestone road, and fish-scale pits road, they all rely on the specific "obstacles" that appear regularly on the roads to achieve the purpose of accelerated test. The geometric characteristics of the road obstacles determine the form and strength of the impact on vehicles. Due to the sensitivity and importance of the geometric characteristics of road obstacles on vehicle, even for the same type of strengthened test road, the roads with different geometric characteristics will have different effects on vehicles. Therefore, for the reconstruction of these roads, the geometric characteristics of the roads can be reconstructed accurately, and they can be better applied to road simulation or virtual test.

Therefore, taking the cobblestone road as the research object, the paper mathematically describes its geometric characteristics and establishes the 3D road model of cobblestone road based on the determination of its key geometry or distribution parameters. To achieve the effect of real road simulation, a more real 3D road model is obtained by integrating the theoretical model with the generated 3D random road. Then the comparison between modeling road and real road is done in space domain and frequency domain. Finally, the influence of cobblestone road geometric parameters on vehicle response is analyzed by establishing standardized vehicle model and evaluation indicators based on the existing 3D road model. The proposed method realizes fast 3D modeling of roads with different parameters and provides the 3D road model with adjustable parameters and real accuracy for building vehicle virtual test ground and carrying out virtual driving test

2. 3D Modeling of Cobblestone Road

The cobblestone road is a kind of strengthened test road by placing the cobblestones with a certain grain size into the cement concrete sparsely and irregularly. The cobblestone road is the most used reliability/durability test road, which can provide a wide band of strong load for the whole vehicle (especially the steering system).

Compared with other strengthened test roads, the 3D modeling of cobblestone road is more complicated because of the random variation in the main parameters such as cobblestone size, cobblestone height, cobblestone distribution, and the shape of cobblestone itself. In this section, based on the exponential 2D oval equation, the 3D model of cobblestone road is gradually established according to the order of Oval curve, cobblestone mode, cobblestone coordinates, and cobblestone road.

2.1. Oval Equation. The exponential oval equation evolves from the standard form of elliptic equation, which can be expressed as

$$\frac{x^2}{a^2} + \frac{y^2}{b^2} e^{kx} = 1 \tag{1}$$

Obviously, when $k = 0$, (1) is a standard form of elliptic equation, where a and b ($a \geq b > 0$) are the length of the semi-axis in the horizontal and vertical directions, respectively. When $k \neq 0$, due to the interference of e^{kx}, for the same abscissa x, the ordinate y becomes the "contraction" end when $kx > 0$ and the value of y is less than the value in the case of the ellipse. Conversely, the ordinate y becomes the "expansion" end when $kx < 0$ and the value of y is larger than the value in the case of the ellipse. Figure 1 shows the oval curves when k are 0.1, 0.2, 0.5, and 0.9 (when k is negative, the figure is symmetrical with the image of Figure 1, which is large in right and small in left).

As shown in Figure 1, k directly determines the shape of the curve, which is called the shape parameter. When k gradually increases from 0, the curve changes from the ellipse to the oval and then cone. In order to maintain the curve to be

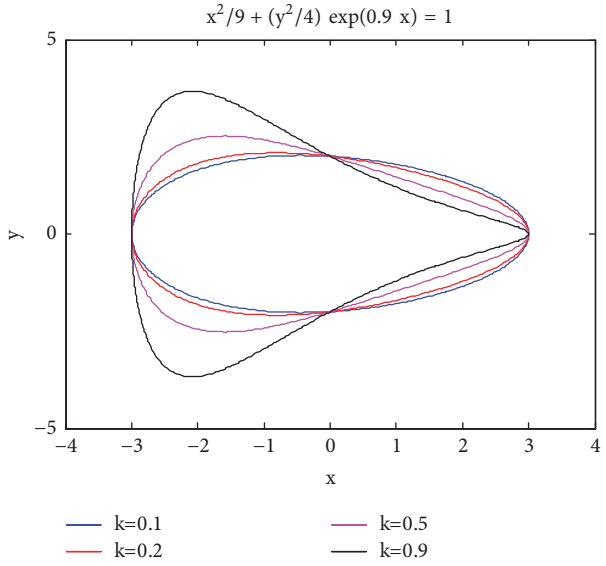

Figure 1: Oval curves under different shape parameters.

used to simulate the cobblestone road, the shape parameter k can be taken to a smaller value.

Obviously, (1) and Figure 1 show that the "height" h in the oval equation is not consistent with the longitudinal semiaxis b in the elliptic equation. When considering the above oval as the vertical section of cobblestone, for the cobblestone with a given height h and particle size $2a$, in order to model with the exponential oval curve expressed in (1), the determined height h is needed to convert to an unknown equivalent semiaxis length b_h when the shape parameter is given. The relationship between them can be derived from (1), which can be expressed as

$$y^2 = \frac{\left(1 - x^2/a^2\right) b^2}{e^{kx}} \tag{2}$$

Taking the derivative of (1) with respect to x, we obtain

$$\frac{dy^2}{dx} = \frac{-2\left(b^2 x/a^2\right) e^{kx} - \left(1 - x^2/a^2\right) b^2 k e^{kx}}{e^{2kx}} \tag{3}$$

When y takes the maximum value of h, there should be $dy^2/dx = 0$. It can be shown from (3) that

$$kx^2 - 2x - ka^2 = 0 \tag{4}$$

According to the solution of (4), when y takes the maximum value of h, its transverse coordinate x can be computed as

$$x = \frac{1 \pm \sqrt{1 + k^2 a^2}}{k} \tag{5}$$

Because $-a \le x \le a$, we have $x = (1 - \sqrt{1 + k^2 a^2})/k$. Then plug it into (1) with $y = h$ at this time, and (1) is rewritten as

$$\frac{\left(\left(1 - \sqrt{1 + k^2 a^2}\right)/k\right)^2}{a^2} + \frac{h^2}{b^2} e^{1 - \sqrt{1 + k^2 a^2}} = 1 \tag{6}$$

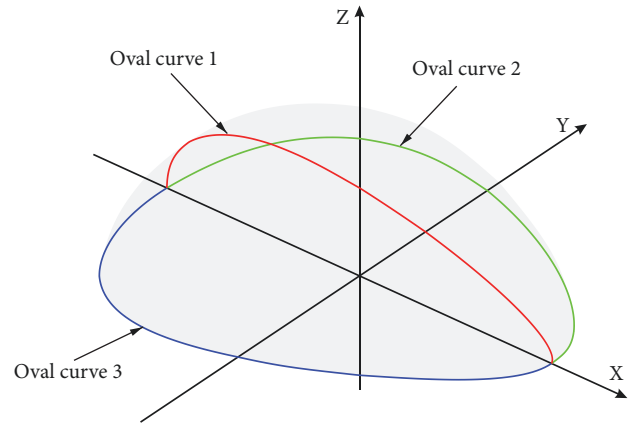

Figure 2: The coordinate system of 3D cobblestone model.

The solution of (6) can be obtained:

$$b_h = ah\,|k| \sqrt{\frac{1}{2} \frac{e^{1 - \sqrt{1 + k^2 a^2}}}{\sqrt{1 + k^2 a^2} - 1}} \tag{7}$$

The relation between the ordinate and the abscissa of any point in the positive half of the longitudinal section can be expressed by plugging (7) into (2).

$$y = \sqrt{\frac{\left(1 - x^2/a^2\right) b_h^2}{e^{kx}}} \tag{8}$$

Equations (7) and (8) form the relation between the transverse and ordinate of the oval curve when the particle size $2a$ and height h are given.

2.2. 3D Cobblestone Model. As shown in Figure 2, for the 3D cobblestone model (aboveground part), three oval equations with the common grain size $2a$ are used as the vertical section, the front/back boundary of the horizontal sections of the cobblestone. Each curve has independent "height" $h_i|_{i=1,2,3}$ (according to the definition, h_2 and h_3 are the maximum particle sizes of the cobblestone along the positive/negative directions of y-axis.) and shape parameter $k_i|_{i=1,2,3}$.

Assume that the XOY plane is the ground. As the boundary of the vertical section, curve 1 determines the actual height and protruding characteristic of the upper part of the cobblestone. And as the boundary of the horizontal section contour, curves 2 and 3 determine the basic shape of the cobblestone.

The oval curves 2 and 3 have independent "height" parameters h_2 and h_3 and the horizontal surface shape parameters k_2 and k_3. Table 1 lists the basic forms of the cobblestone's horizontal surface contour under the conditions of several values of the four parameters. In the actual application process, due to the random change of the particle size in a certain range, a very rich horizontal contour of the cobblestone can be generated under the control of all five parameters.

Table 1: The basic shape of the pebble's horizontal surface profile under different parameters.

	$h_2 < h_3$	$h_2 > h_3$	$h_2 \approx h_3$
$k_2 > k_3 > 0$			
$k_2 \approx k_3 > 0$			
$k_2 > 0 > k_3$			

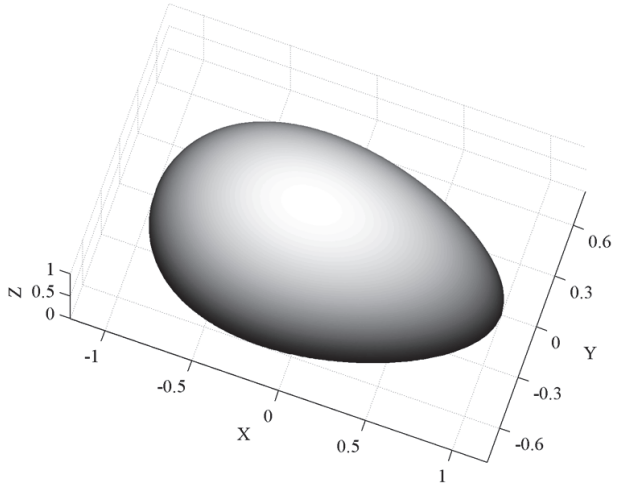

Figure 3: 3D cobblestone model.

When the boundaries expressed by three oval curves are determined, the cobblestone surface consists of the elliptic curves by parallel sliding along the x-axis and connecting the oval curves 1, 2, and 3. The points of the same value x on the oval curves 1, 2, and 3 are used as the end points of semiminor axis and semimajor axis of the ellipse, respectively. Hence, the vertical coordinates of any point on the cobblestone surface corresponding with any point (x, y) on the horizontal surface XOY can be expressed as

$$z(x,y) = \begin{cases} \sqrt{\left(1 - \dfrac{y^2}{y_2^2(x)}\right) z_1^2(x)} & y \geq 0 \\ \sqrt{\left(1 - \dfrac{y^2}{y_3^2(x)}\right) z_1^2(x)} & y < 0 \end{cases} \tag{9}$$

where $z_1(x)$, $y_2(x)$, and $y_3(x)$ denote the points on curves 1, 2, and 3, respectively. They are calculated in the plane of XOZ (replace y with z at this time) and XOY according to (7) and (8).

When $a = 1$, $h_1 = 1$, $h_2 = h_3 = 0.6$, $k_1 = 0.2$, and $k_2 = k_3 = 0.4$, the 3D cobblestone model generated by the above method is shown in Figure 3.

2.3. Center Point Coordinates of Cobblestone. After determining the method of generating 3D cobblestone, they should be scattered on the road randomly according to a certain distribution law. Usually, the intervals between cobblestones are required on the cobblestone road, and it is hoped that the cobblestones can be evenly distributed on the road. Besides, the cobblestones cannot overlap and accumulate obviously.

To simplify the analysis, the horizontal area of all the cobblestones is considered to be a circle with a diameter that varies from the minimum particle size $2a_{\min}$ to the maximum particle size $2a_{\max}$.

When the length L and width W of the road rectangular part are designated and the bottom left corner is defined as the coordinate origin, the above constraint conditions can be expressed as

$$\begin{aligned} d_{ij} &\leq r_i + r_j + D_{\min} \\ r_i &\leq x_{center-i} \leq L - r_i \\ r_i &\leq y_{center-i} \leq W - r_i \end{aligned} \tag{10}$$

where $(x_{center-i}, y_{center-i})$ is the center coordinate of cobblestone i. Both r_i and r_j represent the circle radius of the cobblestones i and j.

$d_{ij} = \sqrt{(x_{center-i} - x_{center-j})^2 + (y_{center-i} - y_{center-j})^2}$ is the distance between the cobblestones i and j.

$D_{\min}$ is the minimum interval between the cobblestones, which can theoretically be obtained in a large range of 0 to $L - 4a_{\min}$. But the value is generally between 0 and 1 m according to the actual test requirements.

However, even if it is simplified as circular, essentially, filling a number of circles with variable radius and without overlapping in a rectangle with a fixed boundary is still a classic Packing problem [22]. From the difficulty of solving this problem, it belongs to the typical Nondeterministic Polynomial (NP) problem [23]. When the number of fillings is large, there is still no ideal method to obtain the deterministic optimal solution at present. However, the cobblestone road itself has no optimal plan for the number of cobblestones (such as filling the specified number of cobblestones in the designated road area), and the optimal solution of the problem is usually arranged in order, which is not consistent with the requirement of cobblestone road. Therefore, the Monte Carlo stochastic search method [24] is used to get the general solution of the problem, which satisfies the situation with as many cobblestone center points as possible of (10). The basic steps of the search method are shown in Figure 4.

As shown in Figure 4, $N_{\max}$ is a maximum allowable value for an attempt to search set in advance. Due to the NP problem, in order to ensure the ergodicity of search, the value must increase sharply with the increase of road area, which is not conducive to rapid modeling. Therefore, when a long road modeling is needed, a complete road model can be established by means of piecewise modeling and then stitching.

When the maximum particle size of 300 mm and the minimum particle size of 150 mm are determined, Figures 5(a) and 5(b) show the results of the cobblestones distribution obtained by Monte Carlo search with the minimum interval of 0 mm and 300 mm in the road range of 10 m × 2 m, respectively.

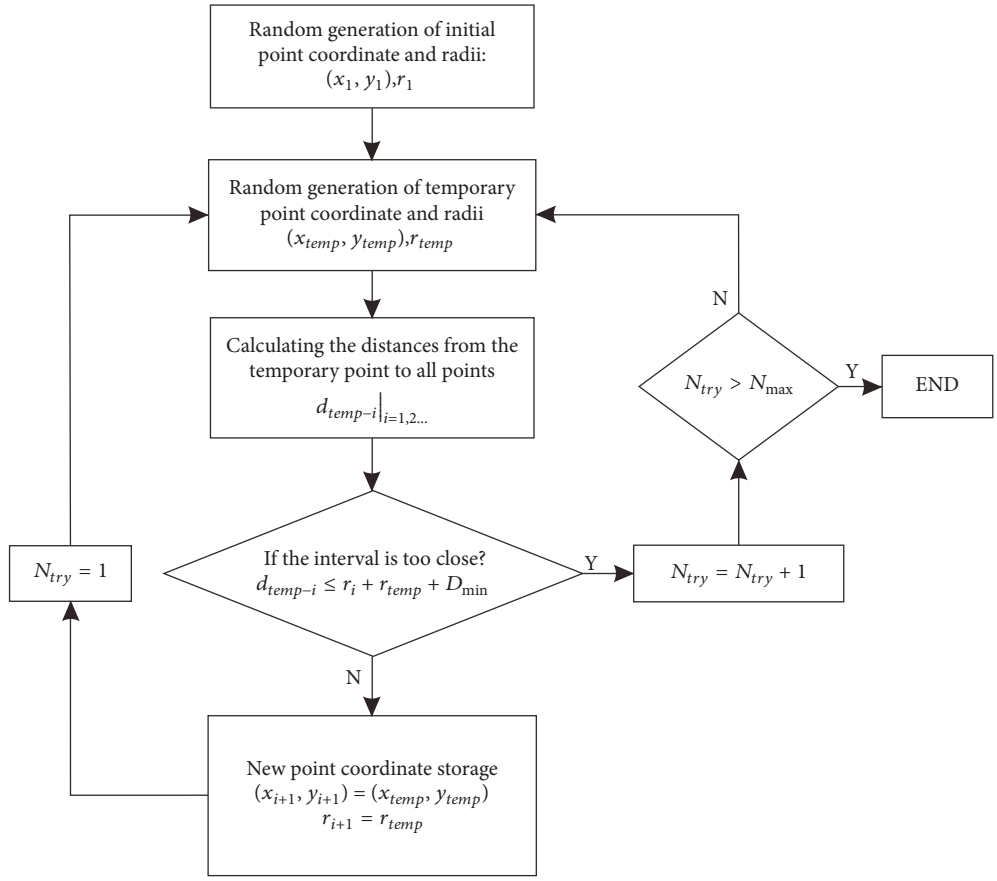

Figure 4: Flowchart of Monte Carlo searching for cobblestone center point.

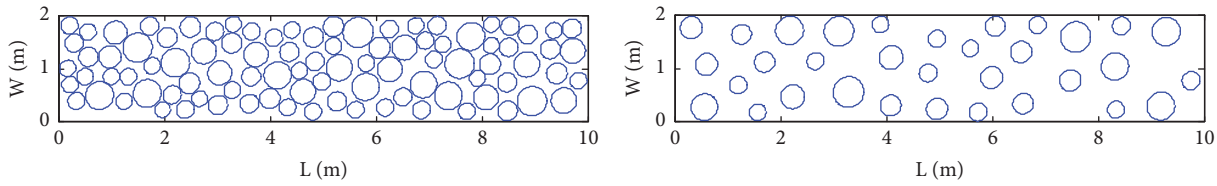

Figure 5: Monte Carlo search results of the cobblestones distribution with different minimum intervals: (a) $D_{\min} = 0mm$; (b) $D_{\min} = 300mm$.

2.4. Plane Rotation and Coordinate Transformation of Cobblestone. From (1) and Figure 1, it is not difficult to find that the maximum size of the cobblestone defined by (7) and (8) is always on x-axis of the coordinate system. If the direction of cobblestone coordinate system is consistent with the direction of the road, all the cobblestones always refer to the length direction of the road. Obviously, to simulate the real cobblestone road, every cobblestone should be assigned a rotating angle around z-axis within the range of $[-90^\circ, 90^\circ]$ before the actual inlay into the road.

The center point coordinate of the cobblestone $(x_{center-i}, y_{center-i})$ shown in Figure 5 has been obtained in the upper section, and the cobblestone coordinate system shown in Figure 2 and the road coordinate system produce the angle θ_i with the rotation operation. Then when the coordinate of the road (x, y) is within the circular area of cobblestone i ($\sqrt{(x - x_{center-i})^2 + (y - y_{center-i})^2} \le r_i$), the coordinate transformation of the original coordinate of the cobblestone $(x'_{center-i}, y'_{center-i})$ can be expressed as

$$\begin{bmatrix} x'_i \\ y'_i \end{bmatrix} = \begin{bmatrix} \cos(\theta_i) & -\sin(\theta_i) \\ \sin(\theta_i) & \cos(\theta_i) \end{bmatrix} \begin{bmatrix} x - x_{center-i} \\ y - y_{center-i} \end{bmatrix} \quad (11)$$

At this time, because (x', y', z') satisfies the equation of 3D cobblestone surface defined by (7), (8), and (9), the height of the cobblestone in the road coordinate system is calculated: $z(x, y) = z'(x', y')$.

The change of the coordinate system (grid) after the cobblestone rotation is shown in Figure 6.

Table 2: The parameters of the cobblestone roads in a vehicle test field.

	Particle size (mm)	Spacing (mm)	Height (mm)	Density (a/m^2)
Cobblestone road A	250~350	≥particle size	80~120	3.5
Cobblestone road B	150~300	200~400	<120	/
Cobblestone road C	70~80	100~200	20~35	30~35

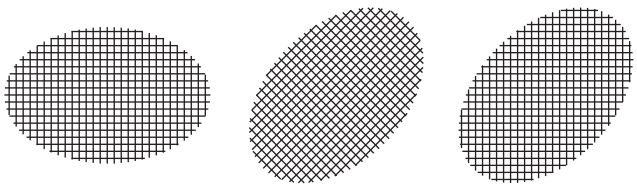

Figure 6: The coordinate system of cobblestones before and after rotation.

2.5. 3D Cobblestone Road. For any point on the cobblestone road, its height can be expressed as

$$z(x,y) = \begin{cases} z_i\left(x_i', y_i'\right) & (x,y) \subseteq S_i \\ 0 & (x,y) \notin S_i \end{cases} \tag{12}$$

where S_i represents the horizontal area surrounded by curves 2 and 3.

As there are many road parameters of the cobblestone road, the road with different emphasis can be produced by the combination of different parameters. Here 3D models of three types of cobblestone roads are built by copying them from a domestic vehicle test ground. The shape and distribution parameters of the three kinds of cobblestone roads in the test ground are shown in Table 2.

As shown in Table 2, for the distribution of cobblestone, the distribution density of cobblestone is required for cobblestone roads A and C except for spacing requirement. In fact, both of them and particle size of the cobblestone are mutually restrictive. As the spacing adjustment is more flexible, the minimum spacing should be adjusted to meet the density requirement first when the distribution density is required.

Besides, among the parameters mentioned in Table 2, the systematicness explanation of the cobblestone (shape parameters $k_{1,2,3}$) is not given. Based on the requirements of particle size and height, the shape parameters are determined as follows.

Road A has the largest diameter, height, and moderate difference in height, and the road is mainly used for the assessment of heavy vehicles. So the shape parameter of the required cobblestone is large, resulting in maximum difference in shape to give the highest strength assessment of vehicle.

Road B has maximum difference in height and larger particle size, so larger vertical shape parameters k_1 and moderate horizontal surface shape parameters $k_{2,3}$ are used to provide abundant lateral change incentives for vehicles with great height difference.

The cobblestone of road C is nearly spherical or hemispherical with small particle size and high density, so the shape parameter of cobblestone has almost no impact on vehicle excitation. The road provides rich high frequency excitation for medium or light vehicles at high speed, so smaller shape parameter is selected.

The 3D cobblestone road models with the length of 10 m and the width of 4 m according to the above parameters by the proposed method are shown in Figure 7.

3. 3D Random Road Fusion

Although the 3D road model of cobblestone road has been established based on the mathematical description of the geometric characteristics, the 3D model is only a theoretical model of the cobblestone road, and there is still a big gap with the actual road. Therefore, based on the theoretical model of 3D cobblestone road, the 3D road model similar to the actual road is obtained by fusing a generated 3D random road with certain road roughness.

3.1. Generation of 3D Random Road. Among the existing methods of generating 3D random road model [25], the harmonic superposition method is the most widely used, which is extended from 2D random standard road model. Based on the random ergodic characteristics of road roughness, the random signal of road roughness is decomposed into a series of sine waves with different frequencies and amplitudes by discrete Fourier transform. For any point in which the road surface coordinate is (x, y), the road roughness in the 3D space can be expressed as

$$q(x,y) = \sum_i \left(\sqrt{2G_d(n_{mi})\,\Delta n} \cdot \sin\left[2\pi n_{mi} F(x,y) + \theta(x,y)\right] \right) \tag{13}$$

where n_{mi} is the central frequency point of frequency band i when the spatial power spectral density (PSD) $G_d(n)$ is divided into several bands with Δn as the resolution, and its corresponding power spectrum value is $G_d(n_{mi})$. $F(x, y)$ is a function that is related to the length/width of the road and its power is 1 and we may as well take $F(x, y) = \sqrt{x^2 + y^2}$ here. $\theta(x, y)$ is a random sequence in $[0, 2\pi]$ changig with (x, y) that satisfies a uniform distribution.

According to the standard ISO/DIS 8608 and GB/T 7031-2005, the road roughness is divided into eight levels by the road PSD, that is, Grade A to H. Considering that the actual test road itself is generally good pavement in addition to obstacles, the road of Grade A (at this time, there is $G_d = (16 \times 10^{-6}) \cdot (n/n_0)^{-2}$, and $n_0 = 0.1m^{-1}$) is used as the random road model fusing with the cobblestone road model. According to the actual design parameters of the cobblestone

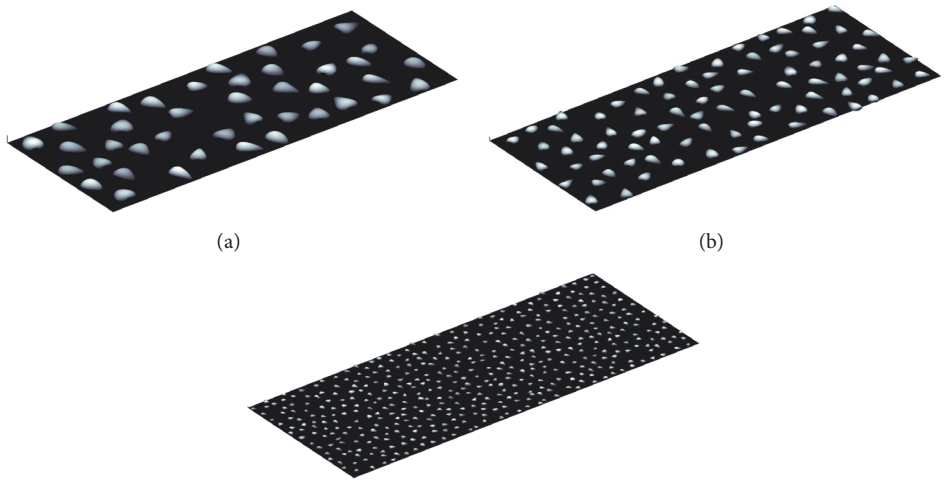

Figure 7: Three kinds of 3D cobblestone road models in a test field. (a) Cobblestone road A. (b) Cobblestone road B. (c) Cobblestone road C.

Figure 8: 3D random road model of Grade A.

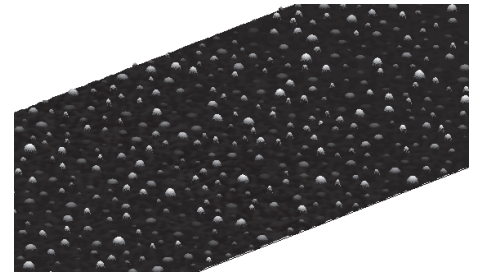

Figure 9: 3D cobblestone road after random road surface fusion.

road, the road grade of the fusion random road model can be adjusted. The standard random road model of Grade A according to (13) is shown in Figure 8.

3.2. 3D Random Road Fusion. For the theoretical road height $z(x, y)$ of cobblestone road and the generated random road $q(x, y)$ above both defined by the horizontal coordinate (x, y), the two 3D road models can be directly fused when the grid coordinates between them are consistent.

Because the cobblestone surface of the cobblestone road itself is more smooth, the fusion is carried out by alternating values between the cobblestone theoretical height $z(x, y)$ and the generated random road height $q(x, y)$. At this time, the real 3D road height according to (12) and (13) can be expressed as

$$z(x, y) = \begin{cases} z_i\left(x_i', y_i'\right) & (x, y) \subseteq S_i \\ q(x, y) & (x, y) \notin S_i \end{cases} \quad (14)$$

The 3D cobblestone road model after the fusion of 3D random road is shown in Figure 9.

The road model generated by the proposed method gives the X, Y, and Z coordinate values of all space points on the road; then the model is usually saved as a text file (or Excel file) in the form of 3D coordinate dot array. In order to apply the 3D road model to virtual simulation test, the 3D road model can be imported into the virtual simulation environment such as Virtual.Lab and Adams and used as a "road model" that can be identified by the simulation environment. Due to the cobblestone road being rigid road, the deformation of the road is negligible. Then the friction coefficient and other parameters are given on the surface of the road model in the virtual environment, and the simulation test research can be carried out.

3.3. Comparison between Modeling Road and Real Road. When the vehicle runs through the cobblestone road, the contact between the tire and the road is a surface contact, which includes not only the tire deformation along the road but also the deformation along the width of the tire. At this time, the excitation input of the road on the vehicle can be regarded as the average of the road roughness on the whole contact surface. However, when the road is long enough, any road trajectory of cobblestone road has the same statistical characteristics in time and frequency domains, which can

Figure 10: The real cobblestone road in picture.

be compared to verify the accuracy of the cobblestone road model established in the paper. Therefore, a real cobblestone road with the similar geometric characteristics in a proving ground is used for comparison with the cobblestone road model, as shown in Figure 10.

Then, using a road profile acquisition system, the road profile of the real cobblestone road is obtained, and the local road profile is shown in Figure 11(a). Similarly, a road trajectory is extracted from the model in the direction of the road on the basis of the established 3D cobblestone road model, and the local road profile is shown in Figure 11(b). The convex parts of the road curve are the cobblestones, and their heights above the ground are mostly concentrated in the range of 20-40 mm.

Because the road profile is usually described in the form of PSD, the PSD of the road profiles in real and modeling cobblestone roads both need to be calculated through Fast Fourier Transform (FFT) for comparison, as shown in Figure 12. Besides, eight standard road spectra from Grade A to Grade H according to ISO/DIS 8608 have been plotted as references. As shown, the road profile of the 3D cobblestone road model mainly concentrates on Grades D, E, and F, which conforms to the real cobblestone road.

4. Analysis of Road Geometric Parameters on Vehicle Response

Based on the establishment of the 3D cobblestone road model, the influence mode of the cobblestone road geometric parameters on the vehicle response is discussed preliminarily by establishing the standardized vehicle vibration model and evaluation indices.

4.1. IRI Standardized Vehicle Model. In the field of road engineering, the International Roughness Index (IRI) is the most widely used quality evaluation index for road [26]. The calculation of IRI is based on a 1/4 vehicle vibration model, as shown in Figure 13(a).

According to Figure 13(a), the dynamic differential equations of the vehicle model can be set up as follows:

$$\begin{aligned} m_s\ddot{z}_s + c_s\left(\dot{z}_s - \dot{z}_u\right) + k_s\left(z_s - z_u\right) &= 0 \\ m_s\ddot{z}_s + m_u\ddot{z}_u + k_t\left(z_u - \overline{q}\right) &= 0 \end{aligned} \tag{15}$$

where z_s and z_u are the vertical displacements of sprung mass and unsprung mass, respectively. $\dot{z}_s$, $\dot{z}_u$, $\ddot{z}_s$, and $\ddot{z}_u$ are vertical velocities and accelerations of sprung mass and unsprung mass, respectively. $\overline{q}$ is the input of the road height by sliding average (the length of the sliding average is the tolerance of the tire to the ground which is B). The sprung mass m_s is used as normalization in the model; then the unsprung mass is $m_u = 0.15m_s$, tire stiffness is $k_t = 653m_s$, suspension stiffness is $k_s = 63.3m_s$ with the unit of N/m, and suspension damping is $c_s = 6m_s$ with the unit of N/ms^{-1}. The width of tire containment is $B = 250mm$. The frequency response curves of the standard model can be calculated by the above parameters, as shown in Figure 13(b).

The longitudinal height on arbitrary abscissa of the established strengthened test road (cobblestone road) is used as the road profile input of the standard vehicle model; then the vehicle responses are obtained.

4.2. Evaluation Indices. In the paper, the IRI and the root mean square (RMS) of vehicle body vertical vibration are used as the indices to evaluate the road and its impact on the vehicle, respectively.

4.2.1. IRI. The IRI is the cumulative value of the relative displacement between the sprung mass and the unsprung mass per kilometer when driving on the corresponding road with the excitation of road roughness, expressed by m/km. It is an important index to evaluate road roughness. According to the definition of IRI, when the total length of the road is L (unit km), $z_s(x)$ and $z_u(x)$ are obtained by solving the differential equation group (15); thus the function of the IRI can be expressed as

$$IRI = \frac{1}{L}\int_0^L \left|z_s - z_u\right| dx \tag{16}$$

4.2.2. RMS of Vehicle Body Acceleration. Corresponding to the road profile represented by IRI, the RMS of vehicle body (here is represented by sprung mass) acceleration is the important index of vehicle vibration intensity, and its value is directly related to vehicle reliability and ride comfort. For the vehicle body acceleration $\ddot{z}_s[k]$ in the discrete form, the RMS is defined as

$$RMS_{\ddot{z}_s} = \sqrt{\frac{1}{N}\sum_{k=1}^{N}\ddot{z}_s^2\,[k]} \tag{17}$$

4.3. Analysis of the Geometric Parameters on Vehicle. As shown in Figure 13(b), the IRI model is typical in simulating the vehicle vibration responses. Therefore, the influences of road geometry parameters on vehicle vibration can be evaluated by the vehicle vibration model and the evaluation indices shown in (16) and (17).

Considering that the vehicle/road vibration model represented by (15) can only evaluate the longitudinal and vertical parameters of the road, the cobblestone road is generated here according to the variation range of the parameters in Table 3, and the IRI and $RMS_{\ddot{z}_s}$ are calculated by (16) and (17). The corresponding relationship between the evaluation indices and the road parameters is shown in Figure 14.

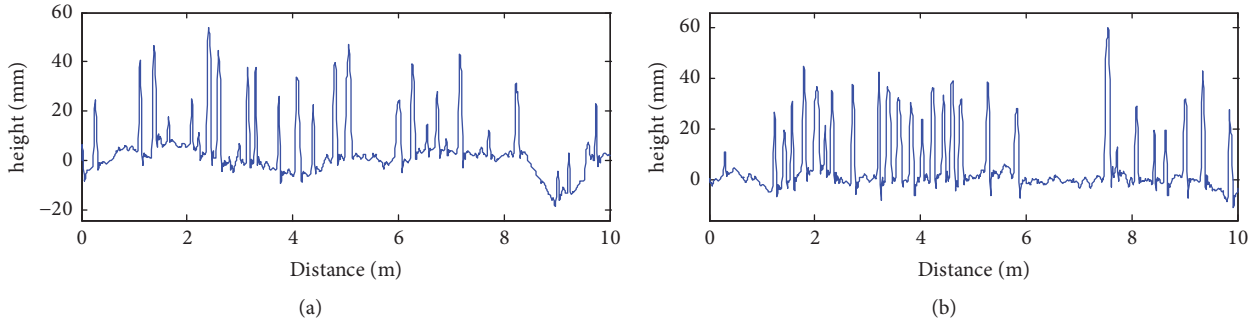

Figure 11: Extracted road profile of cobblestone road. (a) The real road; (b) the modeling road.

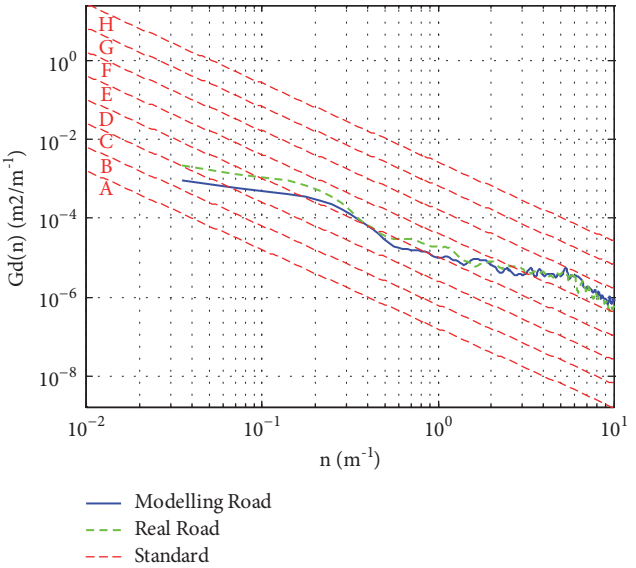

Figure 12: Space PSD of the cobblestone road profile.

As shown in Figure 14, the sizes of the cobblestone on the cobblestone road have a decisive influence on the vehicle vibration, which are mainly reflected in the maximum height h_{max} and the maximum particle size a_{max} of the cobblestone. Both the IRI and the RMS of vehicle body acceleration have a linear relationship with the sizes of the cobblestone. With the increase of the maximum height h_{max} and the maximum particle size a_{max} of the cobblestone, both the IRI and RMS also increase.

The above studies proved that the established road model based on road geometric characteristics can quickly evaluate the effects of various parameters on vehicles and provides useful references for road types and parameters selection when test roads are built.

5. Conclusions

Taking cobblestone road as the research object, a 3D road modeling method based on geometric characteristics is proposed. The oval equation of cobblestone is established and discussed by determining the key geometric characteristics, and the cobblestones distribution on the cobblestone road is determined by Monte Carlo search method. Then the 3D theoretical reconstruction of the cobblestone road is completed, and a generated 3D random road is fused to get a more realistic 3D model of the cobblestone road. The comparison between the modeling road and real road is done in space domain and PSD curves.

Table 3: Geometric parameters of Belgian road and their range of variation.

Road Type	Geometric parameters	Change range/mm
Cobblestone road	Maximum height h_{max}	0~(10-300)
	Particle size a_{min}/a_{max}	20~(50-300)
	Shape parameter k_1	-0.4~0.4
	Interval D_{min}/D_{max}	200~1000

Note: "~" means parameters change randomly in this range; "-" means parameters increase equally in this range.

Based on the standard vehicle vibration model, the IRI and the RMS of vehicle body acceleration are established as the evaluation indices of vehicle vibration, and the influence of key geometric parameters of the cobblestone road on the vehicle vibration was evaluated. Analysis results show that the sizes of cobblestone have a decisive influence on the vehicle vibration.

Although the method proposed in the paper is only verified under the cobblestone road situation, the method is applicable for 3D modeling of almost all strengthened test roads, such as the Belgian road, washboards, and ripple tracks and provides an effective way of 3D road modeling for building vehicle virtual test field.

Abbreviations

3D: Three-dimensional
RGR: Regular Grid Road
CRG: Curved Regular Grid
RDF: Road Definition File
NP: Nondeterministic Polynomial
PSD: Power spectral density
FFT: Fast Fourier Transform
IRI: International Roughness Index
RMS: Root mean square.

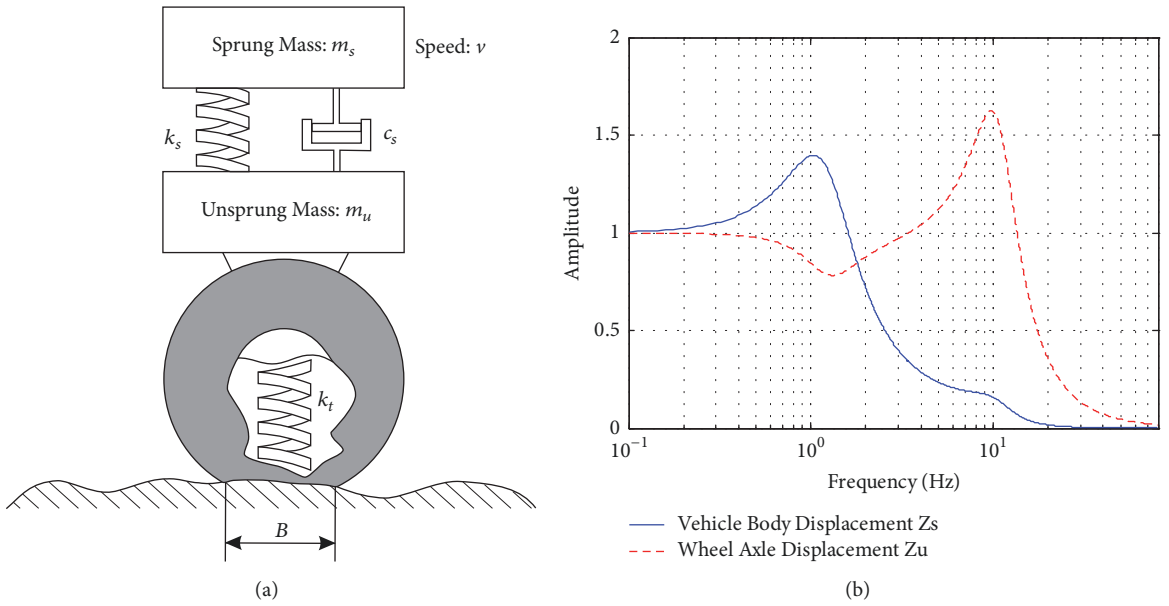

Figure 13: IRI standard vehicle model and its frequency response curves. (a) 1/4 vehicle vibration model. (b) The frequency response curves of the standard vehicle model.

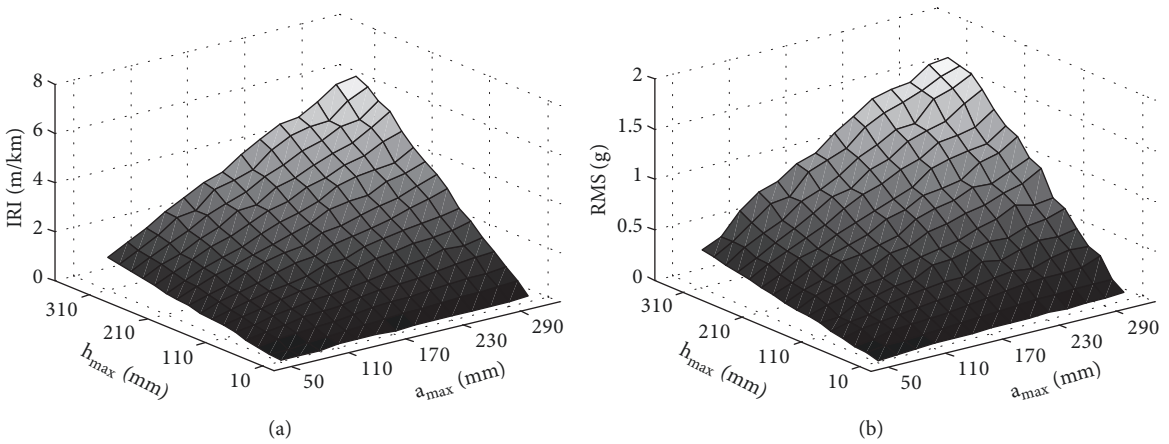

Figure 14: Effect of maximum height and longitudinal length of cobblestones on *IRI* and $RMS_{\ddot{z}_s}$ in cobblestone road. (a) IRI; (b) RMS.

Conflicts of Interest

The authors declare that there are no conflicts of interest regarding the publication of this paper.

Acknowledgments

This work is supported by Weapon and Equipment Exploration Research Project (no. 7131255).

References

[1] A. Halfpenny and M. Pompetzki, "Proving Ground Optimization and Damage Correlation with Customer Usage," *SAE International Journal of Materials and Manufacturing*, vol. 4, no. 1, pp. 620–631, 2011.

[2] P. Xu, W. Dan, P. Leblanc, and G. Peticca, "Road Test Simulation Technology in Light Vehicle Development and Durability Evaluation," SAE 2005 World Congress & Exhibition, paper 14, USA, 2005.

[3] A. M. Sharaf, "Real-time assessment of vehicle response in a virtual proving ground," *International Journal of Heavy Vehicle Systems*, vol. 20, no. 2, pp. 174–189, 2013.

[4] P. J. McGetrick, C. Kim, A. Gonzalez, and E. J. Obrien, "Dynamic Axle Force and Road Profile Identification Using a Moving Vehicle," *International Journal of Architecture, Engineering and Construction*, pp. 1–16, 2013.

[5] K. Reza-Kashyzadeh, M. J. Ostad-Ahmad-Ghorabi, and A. Arghavan, "Investigating the effect of road roughness on automotive component," *Engineering Failure Analysis*, vol. 41, no. 3, pp. 96–107, 2014.

[6] W. Wang, H. Liu, and D. Meng, "Research of Method to Acquire Spectrums for Vehicle Simulation Tests Roadway on Roads," *Construction Machinery Equipment*, vol. 44, no. 8, pp. 18–24, 2013.

[7] H.-Y. Wang, Q.-L. Wang, Q. Rui, R.-L. Li, J. Zhang, and T. Luo, "Research on digitized modeling method of riding road of vehicle," *Binggong Xuebao/Acta Armamentarii*, vol. 37, no. 7, pp. 1153–1160, 2016.

[8] Y. Du, C. Liu, D. Wu, and S. Jiang, "Measurement of international roughness index by using Z-axis accelerometers and GPS," *Mathematical Problems in Engineering*, vol. 2014, Article ID 928980, 10 pages, 2014.

[9] P. Johannesson, K. Podgórski, and I. Rychlik, "Modelling roughness of road profiles on parallel tracks using roughness indicators," *International Journal of Vehicle Design*, vol. 70, no. 2, pp. 1–28, 2016.

[10] H. Duan, F. Shi, F. Xie, and K. Zhang, "Summary of research on road spectrum measurement," *Journal of Electronic Measurement and Instrument*, vol. 24, no. 1, pp. 72–79, 2010.

[11] Y. Zhang, "Time Domain Model of Road Irregularities Simulated Using The Harmony Superposition Method," *Transactions of the Chinese Society of Agricultural Engineering*, vol. 19, no. 6, pp. 32–34, 2003.

[12] X. Wang, J. B. Zhao, and J. Z. Wang, "An improved road roughness simulation method based on trigonometric series method," *Applied Mechanics and Materials*, vol. 513-517, pp. 3277–3282, 2014.

[13] Y. F. Zhu and L. Wang, "Research on the Simulation of Random Road Excitation in Time-Domain," *Applied Mechanics Materials*, vol. 739, no. 6, pp. 508–511, 2015.

[14] X. Liu, H. Wang, Y. Shan, and T. He, "Construction of road roughness in left and right wheel paths based on PSD and coherence function," *Mechanical Systems and Signal Processing*, vol. 60, pp. 668–677, 2015.

[15] V. Rouillard, "Statistical models for nonstationary and non-Gaussian road vehicle vibrations," *Engineering Letters*, vol. 17, no. 4, pp. 1–11, 2009.

[16] H. M. Ngwangwa, P. S. Heyns, H. G. A. Breytenbach, and P. S. Els, "Reconstruction of road defects and road roughness classification using Artificial Neural Networks simulation and vehicle dynamic responses: Application to experimental data," *Journal of Terramechanics*, vol. 53, no. 1, pp. 1–18, 2014.

[17] M. Slabej and P. Kotek, "Using of 3D road surface model for monitoring of transverse unevenness and skid resistance," in *Proceedings of the 23rd Russian-Polish-Slovak Seminar on Theoretical Foundation of Civil Engineering, TFoCE 2014*, pp. 475–480, pol, August 2014.

[18] S. Yu, S. R. Sukumar, A. F. Koschan, D. L. Page, and M. A. Abidi, "3D reconstruction of road surfaces using an integrated multi-sensory approach," *Optics and Lasers in Engineering*, vol. 45, no. 7, pp. 808–818, 2007.

[19] C. Cheng, D. F. Wang, and C. D. Li, "Creation of 3- D Virtual Road with ADAMS," *Automotive Engineering*, vol. 28, no. 2, pp. 163–166, 2006 (Chinese).

[20] B. Rong, P. Xiao, J. Zhou, and Y. Liu, "Reconstruction and Comparative Analysis on 3D Virtual Intensified Road in a Proving Ground," *Qiche Gongcheng/Automotive Engineering*, vol. 39, no. 2, pp. 214–231, 2017.

[21] W. K. Fu, "Analysis and Comparison of Modeling Methods of Virtual Belgian Block Road," *Computer Aided Engineering*, vol. 24, no. 5, pp. 10–15, 2015.

[22] A. Lodi, S. Martello, and M. Monaci, "Two-dimensional packing problems: a survey," *European Journal of Operational Research*, vol. 141, no. 2, pp. 241–252, 2002.

[23] NP_(complexity), 2017, https://en.wikipedia.org/wiki/NP_(complexity).

[24] C. Graham and D. Talay, *Stochastic simulation and Monte Carlo methods*, vol. 68 of *Stochastic Modelling and Applied Probability*, Springer, Heidelberg, 2013.

[25] M. Lin, X. W. Zhang, and S. Y. Cheng, "Simulation of General 3D Virtual Stochastic Road Model," *Applied Mechanics Materials*, vol. 50, no. 51, pp. 382–385, 2011.

[26] E. Freitas, C. Freitas, and A. C. Braga, "The analysis of variability of pavement indicators: MPD, SMTD and IRI. A case study of Portugal roads," *International Journal of Pavement Engineering*, vol. 15, no. 4, pp. 361–371, 2014.